Materials Science and Engineering A 527 (2010) 5065–5071

Contents lists available at ScienceDirect

Materials Science and Engineering A

journal homepage: www.elsevier.com/locate/msea

The microstructural basis for the mechanical properties and electrical resistivity of nanocrystalline $Cu–Al_2O_3$

S. Nachum[a], N.A. Fleck[a,*], M.F. Ashby[a], A. Colella[b], P. Matteazzi[c]

[a] *Cambridge University, Eng. Dept., Trumpington St., Cambridge CB2 1PZ, UK*
[b] *CSGI, Via della Lastruccia, 50019 Sesto Fiorentino, Italy*
[c] *MBN Nanomaterialia S.p.A., Via Bortolan 42-A, 31050 Vascon di Carbonera, Italy*

ARTICLE INFO

Article history:
Received 30 July 2009
Received in revised form 12 February 2010
Accepted 23 April 2010

Keywords:
Nanocrystalline alloys
Electrical resistivity
Dispersion strengthening
Shear bands
Nano-indentation

ABSTRACT

The mechanical properties and electrical resistivity of nanocrystalline copper reinforced by 1 vol.% and 5 vol.% of nano-alumina particles have been measured. The composites were prepared by ball-milling and consolidated by a combination of hot extrusion and HIPing. The uniaxial tensile and compressive strengths are comparable for each composite, and an elastic, ideally plastic response is observed. Shear bands, of width a few microns, accompany plastic deformation. A number of microstructural characterisation tools were used to reveal that grain boundary strengthening and dispersion strengthening are the dominant strengthening mechanisms. Nano-indentation measurements reveal a size effect in hardness. The electrical resistivity is almost double that of pure oxygen free copper and this is mainly ascribed to the presence of dissolved iron.

1. Introduction

Materials of high yield strength, hardness and high electrical conductivity are required in a number of engineering applications. Nanocrystalline copper reinforced by fine oxide particles possess these beneficial properties [1–4], exploiting both grain boundary strengthening and dispersion strengthening [5–14]. The high electrical conductivity of copper is preserved because neither the dispersion of particles nor the small grain size greatly degrade it [15]. One way of manufacturing nanocrystalline alloys with fine and stable dispersed oxide particles is by ball-milling and mechanical alloying [16]. Metal powders are mixed and milled with steel balls until a homogeneous dispersion of oxide particles is achieved and the grain size of the copper matrix is refined. This study explores the structure, the mechanical behaviour and the electrical resistivity of nanocrystalline copper reinforced by 1 vol.% and 5 vol.% of nano-alumina particles made in this way.

2. Experimental procedures

2.1. *Material fabrication process*

Ball-milling of powders, followed by hot extrusion and HIPing was used in order to manufacture nanocrystalline copper with a dispersion of 1 vol.% and 5 vol.% alumina. The process steps are as follows:

(i) Powders of 99.5% purity Cu (size range 45–350 μm), 99.4% purity Al (size range 75–350 μm) and 99.6% purity CuO (size range 45–350 μm) were ball-milled in vacuum at room temperature for 9 h using a steel container and steel balls.[1] The volume ratio of balls to powder was 15:1 and the powder size distribution after milling was below 500 μm. Two volume fractions of alumina, 1 vol.% and 5 vol.%, were formed during the high energy milling process by a redox reaction between the Al and the CuO powders, exploiting the reaction [2]: $X\mathrm{Cu} + 3\mathrm{CuO} + 2\mathrm{Al} = (X+3)\mathrm{Cu} + \mathrm{Al_2O_3}$. The Al and CuO powders were in stoichiometric proportion in order to give Al_2O_3 particles dispersed within the Cu matrix, with no residual Al or CuO after the ball-milling operation. The reaction of Al and CuO is highly exothermic ($\Delta H = -1209$ kJ/mol) with a high reaction rate that requires only a few minutes of milling to activate and complete the reaction, see for example [17].

(ii) Following milling, the powders were consolidated to bars of length 38 mm and diameter 16 mm by extrusion under argon at 25 MPa and 900 °C at a rate of 3 mm s^{-1} and an extrusion ratio of 8. This was followed by HIPing[2] in an argon atmosphere for 30 min under a pressure of 100 MPa and at 600 °C.

---

* Corresponding author. Tel.: +44 01223 748240; fax: +44 01223 332662.
E-mail address: naf1@cam.ac.uk (N.A. Fleck).

[1] MBN Nanomaterialia S.p.A. Italy.
[2] CSGI Italy.

0921-5093/$ – see front matter © 2010 Elsevier B.V. All rights reserved.
doi:10.1016/j.msea.2010.04.070

2.2. Microstructure characterisation

The microstructures were probed by Transmission Electron Microscopy (TEM), Scanning Electron Microscopy (SEM) and Atomic Force Microscopy (AFM), as follows:

(i) Bright field and dark field TEM images, TEM diffraction patterns and X-ray spectroscopy mapping were each taken at 300 kV.[3] The TEM samples were prepared from discs mechanically thinned to 20 μm. A droplet of 70% nitric acid and 30% purified water chemically thinned the disks to TEM foils.
(ii) Samples for the high-resolution scanning microscope[4] were polished using a series of polishing powders down to 0.06 μm colloidal silica and were then etched by 4% Nital solution. The samples were imaged in back-scattered and secondary electron modes and were chemically mapped using X-ray spectroscopy. Additionally, samples were probed using an X-ray diffractometer in order to determine the constituent phases.
(iii) An AFM[5] in contact mode was used to measure the size and shape of the copper grains. Samples were prepared in the same manner as for the SEM examination.
(iv) The electrical resistivity of both composites was measured using a four-probe technique[6] and also by an eddy-current technique.[7] The two techniques gave essentially the same values for resistivity.

2.3. Mechanical tests

Micro-indentation and nano-indentation tests, and uniaxial tension and compression tests were performed on specimens machined from the HIPed bar stock. The details are as follows:

(i) Samples for micro-hardness measurement were mechanically polished using a sequence of powders down to 0.06 μm colloidal silica. The samples for nano-indentation were similarly polished and were then electro-polished.[8] The micro-hardness was measured with a Vickers indenter[9] at five different loads (20 N, 10 N, 5 N, 3 N and 1 N); the hardness data reported below were the average values from 10 indentations at each load. Nano-indentation tests were performed with a Berkovich tip[10] at loads between 250 μN and 10 mN. A 5 s ramp time was used for loading and unloading and the peak load was maintained for 2 s. The contact area in each indent test was determined from the unloading stiffness, as suggested by Oliver and Pharr [18].
(ii) Uniaxial tension and compression tests were performed at a quasi-static strain rate of 10^{-3} s^{-1}; in all tests the loading direction was aligned with the extrusion direction. The compression tests were performed on cylindrical specimens, of diameter 3 mm and length 5 mm; the samples were compressed between hardened, polished steel platens lubricated with petroleum jelly. In the tensile tests, dog-bone specimens were used, of 3 mm × 3 mm square cross-section and of gauge length 8 mm; this shape was used in order to facilitate the observation of shear bands. The surfaces of the dog-bone specimens were polished to a mirror finish using 0.06 μm colloidal silica. In order to highlight the size and orientation of the shear bands, final polishing was performed along the direction of loading; consequently, the as-prepared specimens contained a set of light scratches along the axial direction. The tensile (and compression) samples were loaded in a uniaxial, screw-driven test machine; the axial strain was measured using a resistance strain gauge at strain levels below 2% and using a laser gauge at higher levels of strain.

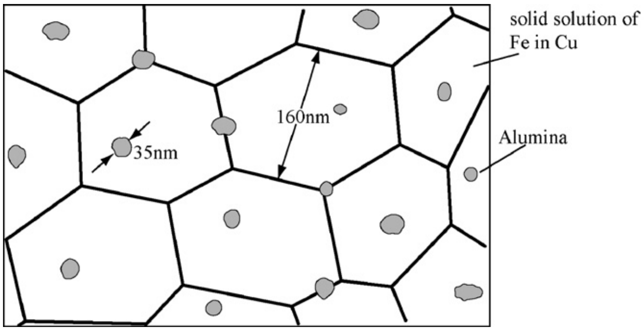

Fig. 1. A sketch of the microstructure.

3. Experimental results

3.1. The observed microstructure

Before detailing the results from each characterisation technique, it is instructive to summarise the observed microstructure of both composites, see the sketch in Fig. 1. Discrete particles of alumina of diameter approximately 35 nm are dispersed within Cu grains of diameter 160 nm; the spacing but not diameter of the alumina particles is dependent upon the volume fraction of alumina phase. Additionally, about 0.1 wt.% Fe, picked up during ball-milling, is dissolved within the Cu grains. There is no evidence for porosity in either composite: the measured densities are in excellent agreement with the theoretical values for full density. The characterisation techniques detailed above gave the following results.

(i) The X-ray diffraction measurements showed strong peaks for Cu and a much smaller peak for alumina. Diffractions from free Al or other phases such as the oxide phases $CuAl_2O_4$, $CuAlO_2$, Cu_2O, CuO, FeO, Fe_2O_3 and Fe_3O_4 were absent. This implies that the dominant phases are Cu and alumina.
(ii) Back-scattered SEM micrographs taken from the 1 vol.% and the 5 vol.% composite are given in Fig. 2(a) and (b), respectively. The grey domains are the Cu grains, whereas the black particles are Al_2O_3 of mean diameter 35 nm.
(iii) Bright and dark field TEM images, diffraction patterns and X-ray spectroscopy mapping have all been employed for both composites. A typical TEM image is given in Fig. 3(a) and the corresponding diffraction pattern is shown in Fig. 3(b) for the 5 vol.% composite; the equivalent images for the 1 vol.% are omitted for the sake of brevity. For both composites, the Cu grain size is 170 nm and alumina particles, of average diameter 40 nm, are located both within the Cu matrix and at Cu grain boundaries. The diffraction rings correspond to copper and alumina phases. X-ray spectroscopy mapping confirmed the presence of Al and O in the stoichiometric proportion of Al_2O_3 [3].
(iv) Topographic images taken by an AFM in contact mode suggested that the Cu grains are equiaxed and of average diameter 160 nm for both compositions of composite. A typical image of the etched surface of the 1 vol.% composite is shown in Fig. 4.

---

[3] Philips CM30.
[4] JEOL 6340F FEGSEM.
[5] Veeco CP-II.
[6] An HP(6612C) digital multimeter.
[7] Hocking Autosigma2000 near-surface eddy current instrument with a 6 mm probe.
[8] Struers LectroPol-5 filled with electrolyte D2.
[9] Shimadzu HMV.
[10] Hysitron Ubi1.